



FINITE ELEMENT IMPLEMENTATION OF DELAMINATION IN COMPOSITE PLATES

Milan Žmindák^{1,*}, Daniel Riecky¹, Martin Dudinský¹

¹ University of Žilina, Faculty of Mechanical Engineering, Department of Applied Mechanics, Univerzitná 1, 010 26 Žilina, Slovak Republic.

*corresponding author: e-mail: milan.zmindak@fstroj.uniza.sk

Resume

Modelling of composite structures by finite element (FE) codes to effectively model certain critical failure modes such as delamination is limited. Previous efforts to model delamination and debonding failure modes using FE codes have typically relied on ad hoc failure criteria and quasi-static fracture data. Improvements to these modelling procedures can be made by using an approach based on fracture mechanics. A study of modelling delamination using the finite element code ANSYS was conducted. This investigation demonstrates the modelling of composites through improved delamination modelling. Further developments to this approach may be improved.

Available online: <http://fstroj.uniza.sk/journal-mi/PDF/2013/03-2013.pdf>

Article info

Article history:

Received 18 May 2012

Accepted 28 August 2012

Online 10 December 2012

Keywords:

Composite structures;
Delamination;
Debonding failure modes.

ISSN 1335-0803 (print version)

ISSN 1338-6174 (online version)

1. Introduction

Composite materials are now common engineering materials used in a wide range of applications. They play an important role in the aviation, aerospace and automotive industry, and are also used in the construction of ships, submarines, nuclear and chemical facilities, etc.

Meaning of the word damage is quite broad in everyday life. In continuum mechanics the term damage is referred to as the reduction of internal integrity of the material due to the generation, spreading and merging of small cracks, cavities and similar defects. Damage is called elastic, if the material deforms only elastically (in macroscopic level) before the occurrence of damage, as well as during its evolution. This damage model can be used if the ability of the material to deform plastically is low. Fiber - reinforced polymer matrix composites can be considered as such materials.

The use of composite materials in the design of constructions is increasing in traditional structures such as development of airplanes, or in the automotive industry.

Recently this kind of materials is used in development of special technique and rotating systems such as propellers, compressor turbine blades, etc. Other applications are in electronics, electrochemical industry, environmental and biomedical engineering [1].

The costs for designing composite structures can be partially or completely eliminated by numerical simulation of a problem. In this case the simulation is not accepted as a universal tool for analyzing systems behaviour but it is an effective alternative to processes of experimental sciences. Simulations support development of new theories and suggestion of new experiments for testing these theories. Experiments are necessary for obtaining input data into simulation programs and for verification of numerical programs and models.

Laminated composites have a lot of advantages but in some cases they show different limitations that are caused by stress concentrations between layers. Discontinuous change of material properties is the reason for

occurrence of interlaminar stresses that often cause delamination failure [2]. Delamination may originate from manufacturing imperfections, cracks produced by fatigue or low velocity impact, stress concentration near geometrical/material discontinuity such as joints and free edges, or due to high interlaminar stresses [3].

Delaminations in layered plates and beams have been analyzed by using both cohesive damage models and fracture mechanics. Cohesive elements are widely used, in both forms of continuous interface elements and point cohesive elements [4], at the interface between solid finite elements to predict and to understand the damage behaviour in the interfaces of different layers in composite laminates. The fracture mechanics approach [5] allows us to predict the growth of a preexisting crack or defect. In a homogeneous and isotropic body subjected to a general loading condition, the crack tends to grow by kinking in a direction such that a pure mode I condition at its tip is maintained. On the contrary, delaminations in laminated composites are constrained to propagate in its own plane because the toughness of the interface is relatively low in comparison to that of the adjoining material. Therefore the delamination crack propagates with its advancing tip in mixed mode condition and consequently requires a fracture criterion including all three mode components.

The theory of crack growth may be developed by using one of two approaches. First, the Griffith energetic (or global) approach introduces the concept of energy release rate (ERR) G as the energy available for fracture on one hand, and the critical surface energy G_c as the energy necessary for fracture on the other hand. Alternatively, the Irwin (local) approach is based on the stress intensity factor concept, which represents the energy stress field in the neighborhood of the crack tip. These two approaches are equivalent and, therefore,

the energy criterion may be rewritten in terms of the stress intensity factors.

Microcracking in a material is almost always associated with changes in mechanical behavior of the material. The problem of microcracking in fiber-reinforced composites is complicated due to the multitude of different microcracking modes which may initiate and evolve independently or simultaneously. Continuum Damage Mechanics (CDM) considers damaged materials as a continuum, in spite of heterogeneity, micro-cavities, and micro-defects and is based on expressing of stiffness reduction caused by damage, by establishing effective damage parameters which represent a cumulative degradation of material. There are basically two categories of CDM models used for estimating the constitutive behavior of composite materials containing microcracks – phenomenological models and micromechanics models.

The phenomenological CDM models employ scalar, second order or fourth order tensors using mathematically and thermodynamically consistent formulations of damage mechanics. Damage parameters are identified through macroscopic experiments and in general, they do not explicitly account for damage mechanism in the microstructure. On the other hand the micromechanics-based approaches conduct micromechanical analysis of representative volume element (RVE) with subsequent homogenization to predict evolving material damage behavior [6]. Most damage models do not account for the evolution of damage or the effect of loading history [7]. Significant error can consequently accrue in the solution of problems, especially those that involve nonproportional loading. Some of these homogenization studies have overcome this shortcoming through the introduction of simultaneous RVE-based microscopic and macroscopic analysis in each load step. However, such approaches can be computationally very expensive since detailed

micro-mechanical analyses need to be conducted in each load step at every integration point in elements of the macroscopic structure.

Jain & Ghosh [7] have developed a 3D homogenization-based continuum damage mechanics (HCDM) model for fiber-reinforced composites undergoing micro-mechanical damage. Micromechanical damage in the RVE is explicitly incorporated in the form of fiber-matrix interfacial debonding. The model uses the evolving principal damage coordinate system as its reference in order to represent the anisotropic coefficients, which is necessary for retaining accuracy with nonproportional loading. The HCDM model parameters are calibrated by using homogenized micromechanical solutions for the RVE for a few strain histories.

There are many works written about damage of composite plates and many models for various types of damage, plates or loading have been developed. In [8] generalized model for laminated composite plates with interfacial damage is presented. This model deals with three kinds of interfacial debonding conditions: perfect bonding, weak bonding and delamination. In [9] unconventional energy based composite damage model for woven and unidirectional composite materials is described. This damage model has been implemented into FE codes for shell elements, with regard to tensile, compressive and shear damage failure modes. Riccio and Pietropaoli [10] have dealt with modeling damage propagation in composite plates with embedded delamination under compressive load. The influence of different failure mechanisms on the compressive behavior of delaminated composite plates was assessed by comparing numerical results obtained with models characterized by different degrees of complexity. Tiberkak et al. [11] have studied damage prediction in composite plates subjected to low velocity impact. Fiber-reinforced composite plates subjected to low velocity impact were studied

by using finite element analysis where Mindlin's plate theory and 9-node Lagrangian element were considered. Clegg [12] has worked out an interesting study of hypervelocity impact damage prediction in composites. This study reports on the development of an extended orthotropic continuum material model and associated material characterization techniques for the simulation and validation of impacts onto fiber-reinforced composite materials. The model allows predicting the extent of damage and residual strength of the fiber-reinforced composite material after impact.

Many studies of an effect of various aspects of damage process on behavior of composite plates can be found in the literature [13]. Many authors have been dealing with problematics of damage of composite plated under cyclic loading or problematics of impact fatigue damage [14]. Composite materials are becoming more and more used for important structural elements and structures, so the problematics of fatigue damage of composites is becoming more and more actual. Numerical implementation of damage is not simple. Finite element method (FEM) is the most utilized method for modeling damage.

The goal of this paper is to present the numerical results of the delamination analysis of two laminae of different thickness with two orthotropic material properties and subjected to a pair of opposed forces. For this goal we have used commercial FEM software ANSYS and the mode I, II, and III components of energy release rate (ERR) were calculated.

2. Theory of failure modeling in laminates

The mechanisms that lead to failure in composite materials are not yet fully understood, especially for matrix or fiber compression. Strength-based failure criteria are commonly used with the FEM to predict failure events in composite structures. Numerous continuum-based criteria have been derived to

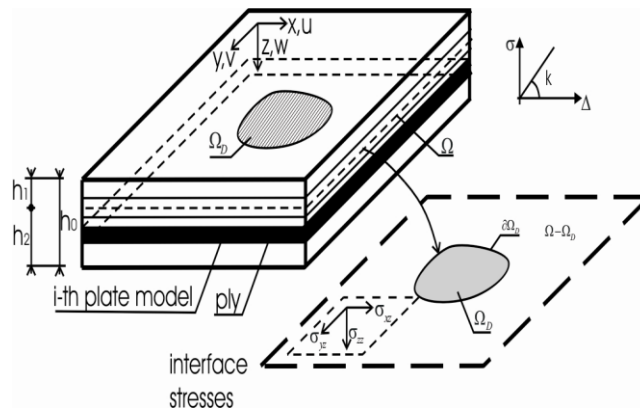


Fig. 1. Delaminated composite plate

relate the internal stresses and experimental measures of material strength to the onset of failure [15]. In Fig. 1 a laminate contains a single in-plane delamination crack of area Ω_D with a smooth front $\partial\Omega_D$. The laminate thickness is denoted by h_0 . The x - y plane is taken to be the mid-plane of the laminate, and the z -axis is taken positive downwards from the mid-plane.

2.1. Plate finite elements for sublaminates modeling

Each sublaminates is represented by an assemblage of the first order shear deformable (FSDT) plate elements bonded by zero-thickness interfaces in the transverse direction as shown in Fig. 2. The delamination plane separates the delaminated structure into two sublaminate of thickness h_1, h_2 and each sublaminates consist the upper n_u plates and the lower n_l plates. Each plate element is composed from one or few physical fiber-reinforced plies with their material axes arbitrarily oriented. Lagrangian multipliers through constraint

equations (CE) are used for enforcing adhesion between the plates inside each sublaminates.

Accordingly, the displacements in the z -th plate element, in terms of a global reference system located at the laminate mid-surface, are expressed [16,17]:

$$\begin{aligned} u_i(x, y, z) &= u_i^0(x, y) + (z - z_i) \psi_{xi}(x, y) \\ v_i(x, y, z) &= v_i^0(x, y) + (z - z_i) \psi_{yi}(x, y) \\ w_i(x, y, z) &= w_i^0(x, y) \end{aligned} \tag{1}$$

where u_i, v_i refer to the in-plane displacements, and w_i to the transverse displacements through the thickness of the i -th plate element, u_i^0, v_i^0, w_i^0 , are the displacements at the mid-surface of the i -th plate element, respectively, and $\psi_{xi}(x, y), \psi_{yi}(x, y)$ denote rotations of transverse normals about y and x axis, respectively.

At the reference surfaces, the membrane strain vector ϵ_i , the curvature κ_i , and transverse shear strain γ_i , respectively are defined as

$$\begin{Bmatrix} \epsilon_{xxi} \\ \epsilon_{yyi} \\ \gamma_{xyi} \end{Bmatrix} = \begin{Bmatrix} \frac{\partial u_i^0}{\partial x} + (z - z_i) \frac{\partial \psi_{xi}}{\partial x} \\ \frac{\partial v_i^0}{\partial y} + (z - z_i) \frac{\partial \psi_{yi}}{\partial y} \\ \frac{\partial u_i^0}{\partial y} + \frac{\partial v_i^0}{\partial x} + (z - z_i) \left(\frac{\partial \psi_{xi}}{\partial y} + \frac{\partial \psi_{yi}}{\partial x} \right) \end{Bmatrix}, \begin{Bmatrix} \kappa_{xxi} \\ \kappa_{yyi} \\ \kappa_{xyi} \end{Bmatrix} = \begin{Bmatrix} \frac{\partial \psi_{xi}^0}{\partial x} \\ \frac{\partial \psi_{yi}^0}{\partial y} \\ \frac{\partial \psi_{xi}^0}{\partial y} + \frac{\partial \psi_{yi}^0}{\partial x} \end{Bmatrix}, \begin{Bmatrix} \gamma_{yzi} \\ \gamma_{xzi} \end{Bmatrix} = \begin{Bmatrix} \psi_{xi}^0 + \frac{\partial w_i^0}{\partial y} \\ \psi_{yi}^0 + \frac{\partial w_i^0}{\partial x} \end{Bmatrix} \tag{2}$$

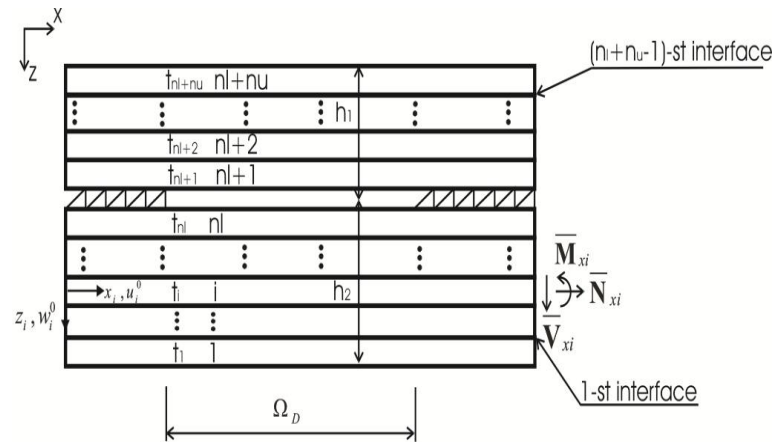


Fig. 2. Laminate subdivision in plate elements

The constitutive relations between the stress resultants and corresponding strains are given in [18]. In this work standard FSDT finite elements available in ANSYS software are used [19]. These elements are joined at the interfaces inside each sublaminates using CE or rigid links characterized by two nodes and three degrees of freedom at each node.

2.2. Interface elements for delamination modeling

Delamination is defined as the fracture of the plane separating two plies of a laminated composite structure [20]. This fracture occurs within the thin resin-rich layer that forms between plies during the manufacturing process. Perfect adhesion is assumed in the undelaminated region $\Omega - \Omega_D$, whereas the sub-laminates are free to deflect along the delaminated region Ω_D but not to penetrate each other. A linear interface model is introduced along $\Omega - \Omega_D$ to enforce adhesion. The constitutive equation of the interface involves two stiffness parameters, k_z, k_{xy} , imposing displacement continuity in the thickness and in-plane directions, respectively, by treating them as penalty parameters. The relationship between the components of the traction vector σ acting at the lower surface of the upper sublaminates, σ_{zx}, σ_{zy} and σ_{zz} , in the out-of-plane (z) and in the in-plane (x and y) directions, respectively, and the corresponding components of relative interface displacement

vector $\Delta, \Delta u, \Delta v$ and Δw are expressed as

$$\sigma = \mathbf{K} \Delta \tag{3}$$

Interface elements are implemented using COMBIN14 type element. Relative opening and sliding displacements are evaluated as the difference between displacements at the interface between the lower and upper sublaminates.

2.3. Contact formulation for damage interface

In order to avoid interpenetration between delaminated sublaminates in the delaminated region Ω_D , a unilateral frictionless contact interface can be introduced, characterized by a zero stiffness for opening relative displacements ($\Delta w \geq 0$) and a positive stiffness for closing relative displacements ($\Delta w \leq 0$), then the contact stress σ_{zz} is

$$\sigma_{zz} = \frac{1}{2} (1 - \text{sign}(\Delta w)) k_z \Delta w \tag{4}$$

where k_z is the penalty number imposing contact constraint and sign is the signum function. A very large value of k_z restricts sublaminates overlapping and simulates the contact condition. Unilateral contact conditions may be implemented in ANSYS using COMBIN39. This element is a unidirectional element with nonlinear constitutive relationships with appropriate specialization of the nonlinear constitutive law according to (4).

If we introduce a scalar damage variable D with the value of 1 for no adhesion and the value 0 for perfect adhesion, we get a single extended interface model with constitutive law valid both for undelaminated $\Omega - \Omega_D$ and delaminated Ω_D areas. Consequently the constitutive law can be expressed as

$$\sigma = (1 - D) K \Delta \quad (5)$$

In this work we use the formulation via FEs, related to plate elements, interface elements and Lagrange multipliers. It is worth noting that in commercial FEA packages the Lagrange multipliers are represented by either CE or rigid links, whereas the interface elements are implemented by the analyst using a combination of spring elements (COMBIN14) and CE.

2.4. Mixed mode analysis

In order to predict crack propagation in laminates for general loading conditions, ERR distributions along the delamination front are needed. Fracture mechanics assumes that delamination propagation is controlled by the critical ERR. Delamination grows on the region of the delamination front where the following condition is satisfied and is in the form of

$$\left(\frac{G_I(s)}{G_I^c} \right)^\alpha + \left(\frac{G_{II}(s)}{G_{II}^c} \right)^\beta + \left(\frac{G_{III}(s)}{G_{III}^c} \right)^\gamma = 1 \quad (6)$$

where α , β and γ are mixed mode fracture parameters determined by fitting experimental test results.

The critical ERR ($G_I^c, G_{II}^c, G_{III}^c$) material properties can be evaluated from experimental procedures. The closed-form expressions for the ERR are [21]

$$G(s) = \frac{1}{2} \lim_{k_z, k_{xy} \rightarrow \infty} [k_z \Delta w^2(s) + k_{xy} \Delta u^2(s) + k_{xy} \Delta v^2(s)], \quad (7)$$

$$\Delta w(s) \geq 0$$

$$G = G_I(s) + G_{II}(s) + G_{III}(s)$$

$$G_I(s) = \begin{cases} \lim_{k_z, k_{xy} \rightarrow \infty} \frac{1}{2} k_z \Delta w^2(s) & \text{if } \Delta w(s) \geq 0 \\ 0 & \text{if } \Delta w(s) < 0 \end{cases} \quad (8)$$

$$G_{II}(s) = \lim_{k_z, k_{xy} \rightarrow \infty} \frac{1}{2} k_{xy} \Delta u_n^2(s)$$

$$G_{III}(s) = \lim_{k_z, k_{xy} \rightarrow \infty} \frac{1}{2} k_{xy} \Delta u_t^2(s)$$

They are obtained by means of the interface model using FE code to check whether propagation occurs. When performing a global FEA of the laminate, then the calculation of $G(s)$ along the delamination front reduces to a simple post-computation. The extent of the propagation of the delamination area may be established by releasing the node in which the relation (6) is first satisfied, leading to a modification of the delamination front, which in turn requires another equilibrium solution. It follows that the delamination growth analysis must be accomplished iteratively. For simplicity, only the computation of ERR is described here. The study of the propagation for a 3D planar delamination requires the use of nonlinear incremental numerical computation.

The delaminated laminate is represented by using two sublaminates (Fig. 2). In this case, the model is called the two-layer plate model. Multilayer plate model in each sublaminates is necessary to achieve sufficient accuracy when the mode components are needed. Sublaminates are modeled by using standard shear deformable elements (SHELL181), whereas interface elements can be used for the interface model. Available interface elements (INTER204) are only compatible with solid elements, therefore interface elements are simulated here by coupling CE with spring elements (COMBIN14). Plate and interface models must be described by the same in-plane mesh.

The FE model of the plates adjacent to the delamination plane in proximity of the delamination front is illustrated in Fig. 3.

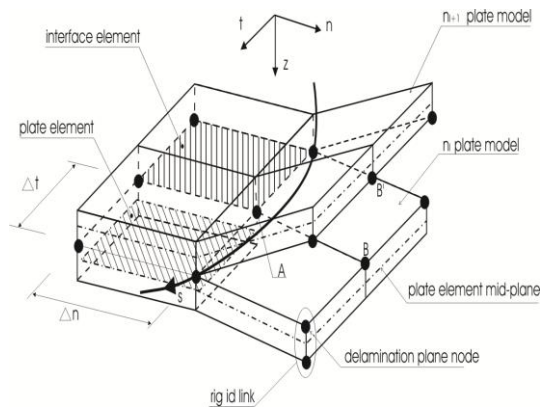


Fig. 3 Plate assembly in the neighborhood of the delamination front

Interface elements model the undelaminated region $\Omega - \Omega_D$ up to the delamination front. The mesh of interface and plate elements must be sufficiently refined in order to capture the high interface stress gradient in the neighborhood of the delamination front, which occurs because high values of interface stiffness must be used to simulate perfect adhesion. The individual ERR at the general node A of the delamination front are calculated by using the reactions obtained from spring elements and the relative displacements between the nodes already delaminated and located along the normal direction.

ERR are computed using (9), which is a modified version of (8) to avoid excessive mesh refining at the delamination front. This leads to the following expressions

$$\begin{aligned}
 G_I(A) &= \left(\frac{1}{2} \frac{R_A^z \Delta w_{B-B'}}{\Delta_n \Delta_t} \right), \\
 G_{II}(A) &= \left(\frac{1}{2} \frac{R_A^n \Delta u_{nB-B'}}{\Delta_n \Delta_t} \right), \\
 G_{III}(A) &= \left(\frac{1}{2} \frac{R_A^t \Delta u_{tB-B'}}{\Delta_n \Delta_t} \right)
 \end{aligned} \tag{9}$$

where R_A^z is the reaction in the spring element connecting node A in the z-direction, $\Delta w_{B-B'}$ is the relative z-displacement between the nodes B and B'. These are located immediately ahead of the delamination front along its normal direction passing through A.

Similar definitions apply for reactions and relative displacement related to modes II and III. The characteristic mesh sizes in the normal and tangential directions of the delamination front are denoted by Δ_n and Δ_t . In (9), the same element size is assumed for elements ahead of and behind the delamination front. Value $\Delta_t/2$ must be used in (9) instead of Δ_t when the node is placed at a free edge.

In order to simplify the FE modeling procedure, it is possible to introduce spring elements only along the delamination front instead of the entire undelaminated region. The perfect adhesion along the remaining portion of the undelaminated region can be imposed by CE. However, when the delamination propagation must be simulated, it is necessary to introduce interface elements in the whole undelaminated region $\Omega - \Omega_D$.

In the next example, the delamination modeling techniques presented so far are applied to analyzing typical 3D delamination problems in laminated plates. The ERR distribution along the delamination front are computed for different laminates and loading conditions.

3. Finite element modeling and numerical example

One of the most powerful computational methods for structural analysis of composites is the FEM. The starting point would be a “validated” FE model, with a reasonably fine mesh, correct boundary conditions, material properties, etc. [22]. As a minimum

requirement, the model is expected to produce stress and strains that have reasonable accuracy to those of the real structure prior to failure initiation.

The results of the delamination analysis of two laminae of different thickness and material are processed in this section. The laminae are fixed on one side and free on the other side. Loads are applied on the free side depending from the analyzed type of delamination (Fig.4).

The upper sublamina has these properties: $E_x = 35000$ MPa, $E_y = E_z = 10500$ MPa, $G_{yz} = 10500$ MPa, $G_{xy} = G_{xz} = 1167$ MPa, $\nu_{xy} = \nu_{xz} = \nu_{yz} = 0.3$. The lower sublamina has these properties: $E_x = 70000$ MPa, $E_y = E_z = 21000$ MPa, $G_{yz} = 2100$ MPa, $G_{xy} = G_{xz} = 2333$ MPa, $\nu_{xy} = \nu_{xz} = \nu_{yz} = 0.3$. The pair of forces applied on the laminae is $T = 1$ N/mm and the dimensions of the laminate are: $a = 10$ mm, $B = 20$ mm, $L = 20$ mm, $h_1 = 0.5$ mm, $h_2 = 1$ mm. The upper sublamina is composed from four plates $n_u = 4$ and the lower by two $n_l = 2$. The plates are meshed by SHELL181 element. The zone of mesh refinement has these dimensions $5 * 20$ mm, it is centered around the delamination front, which is placed in the middle of the laminate. The interface between the sublaminates is modeled without stiffness for opening displacements and with positive stiffness for closing displacements. The interface between sublaminates is modeled by means of CE (Constrain Equation), since it is easier to apply than beam elements and delamination propagation is not solved. The delamination front is created by spring elements COMBIN 14, in each node of the delamination front by three elements.

The stiffness of the spring elements binding the laminae is chosen as k_z and $k_{xy} = 10^8$ N/mm³. These elements are oriented in different directions, they were created always from a pair of nodes placed on the surface of the lower sublamina. One of the pair nodes is bounded to the upper plate by means of CE and the second

one to the lower plate. ERR is calculated by using deformation along the delamination front.

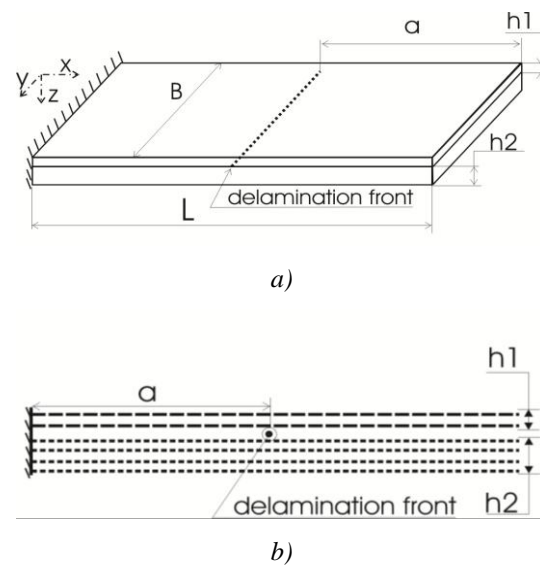


Fig. 4 a) Scheme of boundary conditions and laminate dimensions, b) scheme of FEM model, h_1 simulated by 2 layers, h_2 simulated by 4 layers

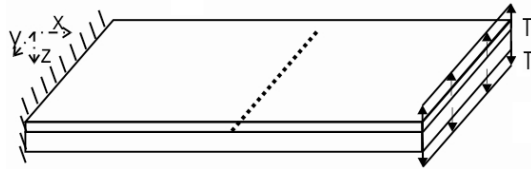
Model I

At model I the ERR for delamination type I is analyzed. Model I is loaded with opening forces T , which are parallel to z axis, of magnitude 1 N/mm, displayed in Fig. 5a. For the calculation of the ERR the equation (9) was used for the type I. As the biggest ERR is in the middle of the model, it is expected that beginning of delamination is in the middle of the model. The distribution of ERR through the width of the laminate is displayed in the Fig. 5b.

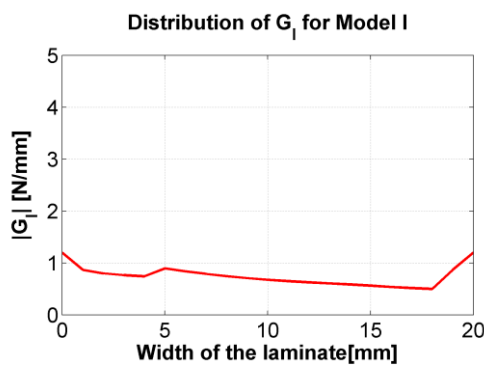
Model II

In this model the sliding type II of delamination was simulated. Applied forces are parallel with the x axis (Fig. 6a). Two types of ERR were analyzed on this model, G_{II} in the x direction and G_{III} in the y direction. ERR was calculated separately for each direction. The reaction of the spring elements are used for the calculation of G_{II} and the y reactions are used for the calculation of G_{III} . Both distributions are displaying the absolute values of ERR, at both distributions are

the values of ERR smaller than the values of G_I . The values of G_{II} are in the range of $(0.5, 2) \cdot 10^{-4}$ and the values of G_{III} are in the range of $(0, 4) \cdot 10^{-6}$ (Fig. 7).

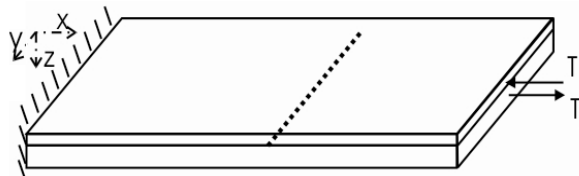


a) Forces applied on the laminate model

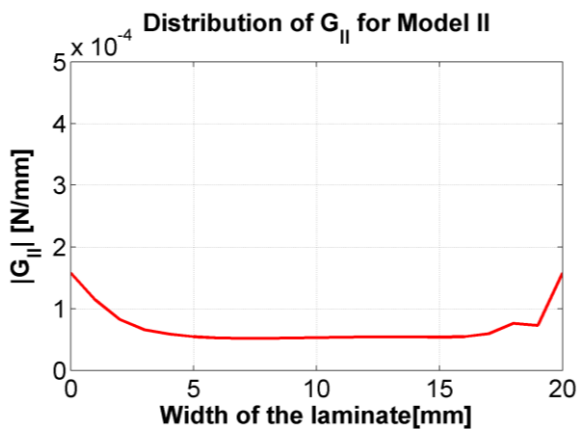


b) ERR distribution for delamination type I of G_I

Fig. 5. Scheme of FEM Model I



a) Direction of loads for type II delamination,



b) distribution of ERR for delamination type II of G_{II}

Fig. 6. Scheme of FEM Model II

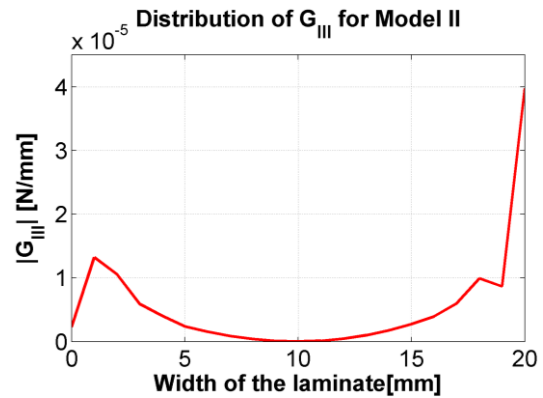
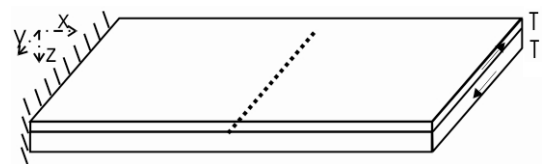
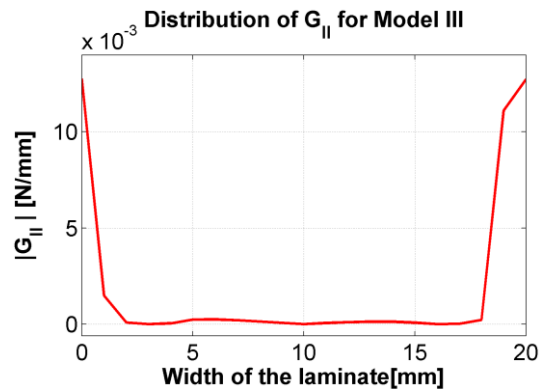


Fig. 7. The distribution of ERR for delamination type II of G_{III}



a) Definitions of loads for delamination type III



b) distribution of G_{II} for model III

Fig. 8. Scheme of FEM Model III:

Model III

At this model the type III of delamination is analyzed, the tearing. Again, the geometry of model I was used, with the mesh and its refinement around the delamination front, boundary conditions and the linking between the plates, but the direction of the applied forces has changed (Fig. 8a). Both types of ERR are analyzed here, G_{II} in the x direction and G_{III} the y direction. The values of ERR are in these ranges: value of G_{II} in the range of $(0, 14) \cdot 10^{-3}$ and the value of G_{III} in the range of $(0, 0.02)$. It is possible that better results could be achieved by increasing the number of plate elements layers simulating the sublamina. These models

can be modeled by solid elements, but there is a greater number of elements needed for accurately simulating the stress and ERR gradients. Thereby the number of equations and computing time increase.

4. Conclusion

Methodology for calculation of delamination of laminate plates was derived in this paper. The analysis shows that when mixed mode conditions are involved, a double plate model to accurately capture accurately the mode decomposition in region near midpoint of the delamination front. The solution converges quickly because a small number of plates is needed to obtain a reasonable approximation.

Acknowledgment

The authors gratefully acknowledge the support by the Slovak Grant Agency VEGA 1/1226/12 and Slovak Science and Technology Assistance Agency registered under number APVV-0169-07.

References

- [1] D. L. Chung, D. L. Deborah: Composite Materials: Functional Materials for Modern Technology, Springer, London 2003.
- [2] Z. Zhang, S. Wang, S.: Composite Struct. 88 (2009) 121-130.
- [3] N. Hu, Elmarakbi, H. Fukunaga: Composites Sci. Technol. 69 (2009) 2383-2391.
- [4] W. Cui, M. A. Wisnom: Composites 24 (1993) 467-474.
- [5] J. Sládek, V. Sládek, L. Jakubovičová: Application of Boundary Element Methods in Fracture Mechanics, VTS University of Žilina, Žilina 2002.
- [6] L. Mishnaevsky: Computational Mesomechanics of Composites, Numerical analysis of the effect of microstructures of composites on their strength and damage resistance. John Wiley and Sons, Wiley online library 2007.
- [7] J. R. Jain, S. Ghosh: Int. J. Damage Mechanics 18(6) (2009) 533-568.
- [8] X. Shu: Composite Struct. 74(2) (1993) 237-246.
- [9] L. Iannucci, J. Ankersen.: Composites Sci. Technol. 66(7-8) (2006) 934-951.
- [10] A. Riccio, E. Pietropaoli: J.Composite Mater. 42(13) (2008) 1309-1335.
- [11] R. Tiberkak: Composite Struct. 83(1) (2008) 73-82.
- [12] R. A. Clegg, D. M. White, W. Riedel, W. Harwick: Int. J. Impact Eng. 33(1-12) (2006) 190-200.
- [13] P. Gayathri, K. Umesh, R. Ganguli: Reliability Eng. Sys. Safety 95(7) (2010) 716-728.
- [14] K. Azouaoui, Z. Azari, G. Pluinage: Int. J. Fatigue 32(2) (2010) 443-452.
- [15] C. G. Dávila, P. P. Camanho, Ch. A. Rose: J. Composite Mater. 39(4) (2005) 323-345.
- [16] E. Carrera: Arch. Comput. Meth. Eng. 9(2) (2002) 87-140.
- [17] J. N. Reddy, A. Miravete: Practical analysis of composite laminates, CRC Press, New York 1995.
- [18] M. Žmindák, D. Riecky, S. Danišovič: Machine dynamics res. 34(1) (2010) 130-138.
- [19] Ansys v.11: Theory manual, ANSYS, Inc., Southpointe, PA 2007.
- [20] M. T. Fenske, A. J. Vizzini: J. Composite Mater. 35(15) (2001) 1325-1342.
- [21] E. J. Barbero: Finite Element Analysis of Composite Materials, CRC Press, Boca Raton 2008.
- [22] K. J. Bathe: Finite Element Procedures, Prentice Hall, New Jersey 1996.